Since January 2020 Elsevier has created a COVID-19 resource centre with free information in English and Mandarin on the novel coronavirus COVID-19. The COVID-19 resource centre is hosted on Elsevier Connect, the company's public news and information website.

Virology 525 (2018) 161–169

Contents lists available at ScienceDirect

Virology

journal homepage: www.elsevier.com/locate/virology

The avian influenza virus PA segment mediates strain-specific antagonism of BST-2/tetherin

Jaraspim Narkpuk, Anan Jongkaewwattana, Samaporn Teeravechyan*

Virology and Cell Technology Laboratory, National Center for Genetic Engineering and Biotechnology, National Science and Technology Development Agency, 113 Thailand Science Park Phaholyothin Rd, Klong 1, Klong Luang, Pathumthani 12120, Thailand

ARTICLE INFO

Keywords:
BST-2
Tetherin
Influenza virus
Avian influenza
PA
PA-X
NS1

ABSTRACT

BST-2 is an antiviral protein described as a powerful cross-species transmission barrier for simian immunodeficiency viruses. Influenza viruses appear to interact with BST-2, raising the possibility that BST-2 may be a barrier for cross-species transmission. An MDCK-based cell line expressing human BST-2 was generated to study human-derived A/Puerto Rico/8/36 (H1N1; PR8) as well as two low pathogenic avian influenza viruses (subtypes H4N6 and H6N1). The H4N6 and H6N1 viruses were less affected by BST-2 expression than PR8, due to their ability to decrease BST-2 levels, a function localized to the PA segment of both avian viruses. Experiments with PA-mutant and -chimeric viruses confirmed that the avian PA segment conferred BST-2 downregulation and antagonism. These results indicate a species-specific ability of PA from low pathogenic avian viruses to mitigate human BST-2 antiviral activity, suggesting that BST-2 is unlikely to be a general cross-species barrier to transmission of such viruses to humans.

1. Introduction

BST-2 (bone marrow stromal cell antigen 2), also known as tetherin, CD317 or HM1.24, is an interferon (IFN)-induced cellular protein that was initially described in 2008 as a restriction factor for human immunodeficiency virus type 1 (HIV-1) (Neil et al., 2008; Van Damme et al., 2008). While BST-2 has been almost exclusively studied as a mammalian antiviral protein, an *in silico* study identified a BST-2 ortholog as far back in vertebrate evolution as the elephant shark, dating the appearance of this gene to over 450 million years ago (Heusinger et al., 2015). Other than in fish, this study also identified orthologs in marsupials, reptiles, and birds, with alligator BST-2 being tested and found to possess antiviral function against HIV-1 release. Among birds, BST-2 was found in turkeys and chickens, but appears to have been lost through gene erosion among many bird species.

As a type II membrane protein, BST-2 possesses a C-terminal GPI (glycophosphatidylinositol) modification and an N-terminal transmembrane domain flanking an extracellular coiled coil central region, and is present on the cell surface as a homodimer (Kupzig et al., 2003). The resulting four-membrane-anchor conformation is considered central to the ability of BST-2 to restrict HIV-1 virion release, where it acts as a "tether" linking the membranes of budded virions to the host cell membrane (Perez-Caballero et al., 2009). As BST-2 acts directly upon the host cell membrane rather than viral components, BST-2 does not target a specific virus but rather has been found capable of restricting virion release and spread for a range of enveloped viruses beyond the retroviruses, such as filoviruses (Jouvenet et al., 2009; Kaletsky et al., 2009; Sakuma et al., 2009), arenaviruses (Radoshitzky et al., 2010; Sakuma et al., 2009), and various coronaviruses (Taylor et al., 2015; Wang et al., 2014).

Many of the viruses described to be sensitive to BST-2 restriction are zoonotic. Most notably, BST-2 has been described as a cross-species transmission barrier that shaped the evolution of the simian immunodeficiency virus (SIV) and HIV (Evans et al., 2010). A recent publication also demonstrated the possible role of BST-2 as a cross-species transmission barrier for various orthobunyaviruses (Varela 2017), with human viruses being restricted by sheep BST-2 but not the human ortholog, and vice versa. Also, equine BST-2 was observed to restrict the growth of both equine and human influenza viruses more effectively than human BST-2 (Wang et al., 2018).

Early reports examining the interplay between influenza viruses and BST-2 suggested that virus-like particles (VLPs) but not wild-type viruses were susceptible to human BST-2 restriction (Watanabe et al., 2011, Bruce et al., 2012). These observations lent credence to the possibility that influenza viruses universally encode an antagonist to BST-2. Contradictory reports soon emerged, however, of viruses inherently sensitive to BST-2 restriction (Gnirss et al., 2015; Hu et al., 2017; Mangeat et al., 2012). Differential abilities of various influenza

* Corresponding author.
E-mail address: samaporn.tee@biotec.or.th (S. Teeravechyan).

https://doi.org/10.1016/j.virol.2018.09.016
Received 16 August 2018; Received in revised form 19 September 2018; Accepted 21 September 2018
Available online 02 October 2018

virus neuraminidases (NA) in circumventing BST-2 activity (Leyva-Grado et al., 2014; Yondola et al., 2011) made it apparent that influenza virus sensitivity to BST-2 is likely to be strain-specific. Further studies supported the possibility that influenza virus NA acts a strain-specific antagonist to BST-2 (Leyva-Grado et al., 2014; Mangeat et al., 2012). Mangeat et al. also reported a reduction in BST-2 protein expression, which may be associated with hemagglutinin (HA) and NA together (Gnirss et al., 2015) or the M2 protein (Hu et al., 2017), but their observations of decreased BST-2 mRNA levels during influenza virus infection remained unexplained. Given the variety of influenza strains, host cells, and methodologies used to study the BST-2–influenza interplay, the conflicting data, at the very least, appear to suggest that a variety of influenza virus strains interact with and counteract BST-2 in some fashion.

Given that influenza is and remains an important zoonotic disease, the possibility of BST-2 being a host restriction factor that acts as a cross-species transmission barrier for avian influenza viruses is intriguing. Thus far, however, studies examining the intersection between BST-2 and influenza viruses have mostly focused on human viruses, whether laboratory-adapted, seasonal, or pandemic. These viruses have been successful in maintaining themselves in the human population, suggesting that they possess an inherent capacity to circumvent or antagonize the antiviral activity of BST-2. Therefore, we were interested in comparing human and low pathogenic avian influenza virus strains, which are generally not deemed a direct threat to human health, with the goal of identifying differences in their response to BST-2.

2. Results

2.1. Generation of BST-2-expressing cell lines

To study the impact of BST-2 on human and avian influenza viruses, we first generated an MDCK cell line stably expressing human BST-2 cloned from HeLa cells (Narkpuk et al., 2014) (Supplementary Fig. 1). The MDCK-BST-2 cell line generated by lentiviral transduction was examined by immunofluorescence staining and BST-2 was observed as punctate clusters on cell surface membranes (Fig. 1A), in accordance with expected BST-2 localization. Cells were also probed for BST-2 expression by western blotting and revealed the characteristic pattern of monomeric and dimeric BST-2 in its various glycosylated forms (Fig. 1B).

2.2. Low pathogenic avian viruses are resistant to human BST-2

To test for strain-specific differences in sensitivity to human BST-2, we compared the low pathogenic avian viruses A/duck/Hong Kong/365/78 (H4N6) and A/duck/Suphanburi/AI157/2005 (H6N1) against A/Puerto Rico/8/34 (H1N1) (PR8 for short). These viruses were used to infect MDCK and MDCK-BST-2 cells at a low multiplicity of infection (MOI), and their supernatants were harvested at 48 h post-infection for plaque titration on MDCK cells. As low pathogenic avian viruses have not been reported to cause disease in humans, we expected that the H4N6 and H6N1 viruses would be more susceptible to human BST-2 antiviral activity than PR8. Surprisingly, the PR8 virus exhibited greater sensitivity to BST-2, with titers decreasing by around 1 log in MDCK-BST-2 cells (Fig. 2A). Neither the H4N6 nor H6N1 virus appeared to be negatively affected by the presence of BST-2, with H4N6 showing a slight trend towards increased replication in MDCK-BST-2 cells (Fig. 2B, C). When infected cells were probed to confirm BST-2 expression, western blotting revealed a dramatic disappearance of BST-2 protein in MDCK-BST-2 cells infected by H4N6 and H6N1 viruses (Fig. 2D). Similar levels of BST-2 protein down-regulation were not observed with PR8 infection prior to complete cell death. Analysis of BST-2 mRNA demonstrated that this reduction was accompanied by reduced mRNA levels as well (Fig. 2E). PR8 infection also resulted in decreased BST-2 mRNA levels, albeit not as drastically as infection with the avian viruses. While this result reflects the ability of influenza A viruses in general to mediate host shut-off (Rivas et al., 2016), it also suggests a difference in mRNA down-regulation that may be associated with decreased levels of BST-2. Alternatively, it is also possible that mRNA and protein down-regulation effects occur through distinct mechanisms.

These avian viruses should not have been under selection pressure to develop a specific antagonistic mechanism against human BST-2, due to the nature of their host range. These observations therefore pointed to a general host response inhibition factor present in the virus. The influenza virus nonstructural protein 1 (NS1), in particular, is known for its ability to inhibit an IFN-induced antiviral state through a variety of activities such as blocking host sensors of viral RNA and signal transduction pathways leading to induction of IFN expression (Marc, 2014). As BST-2 expression in our cell line is driven by a constitutive promoter, however, we do not expect that these particular activities will be involved in BST-2 down-regulation.

2.3. The PA segment encodes a common BST-2 antagonist in avian influenza viruses

To determine which viral factors of H4N6 and H6N1 are involved in decreasing BST-2 levels, we studied the impact of each of their genomic segments on BST-2 expression in the context of transfection. We amplified each segment from viral RNA for cloning into the reverse genetics vector pHW2000. Individual genomic segments of PR8, H4N6, and H6N1 were then co-transfected with a BST-2 expression plasmid into HEK293T cells for western blot analysis. While none of the PR8 genomic segments affected BST-2 expression (Fig. 3A), the PA of H4N6 and H6N1 notably reduced BST-2 protein levels (Fig. 3B, C). Additionally, the H6N1 NS segment also exhibited the capacity to reduce protein expression, which is likely due to NS1-associated host shut-off capabilities (Marc, 2014).

As the effect of the PA segment appeared common to both low pathogenic avian viruses, we further tested the effect of PA on BST-2

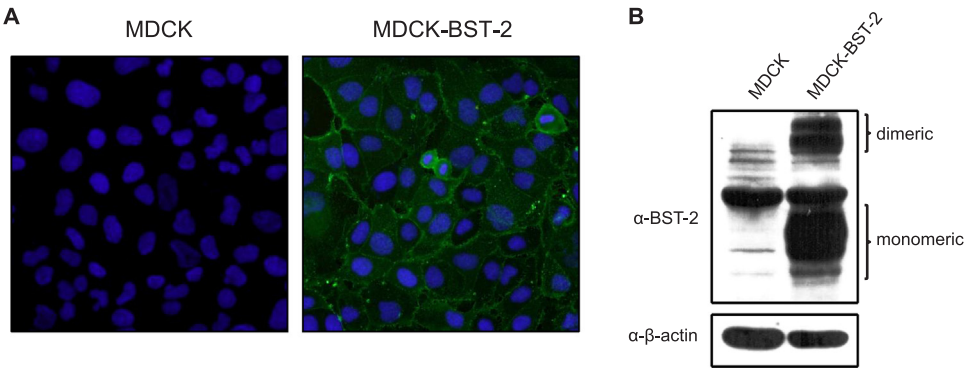

Fig. 1. Expression of the human BST-2 transgene in MDCK cells. (A) MDCK and MDCK-BST-2 cells were fixed with formaldehyde and probed for BST-2 expression (green). Cells were stained with DAPI prior to imaging by fluorescence microscopy. (B) MDCK and MDCK-BST-2 cells were plated in 6-well plates and subsequently harvested. Cell lysates were analyzed by western blotting for BST-2 and β-actin expression.

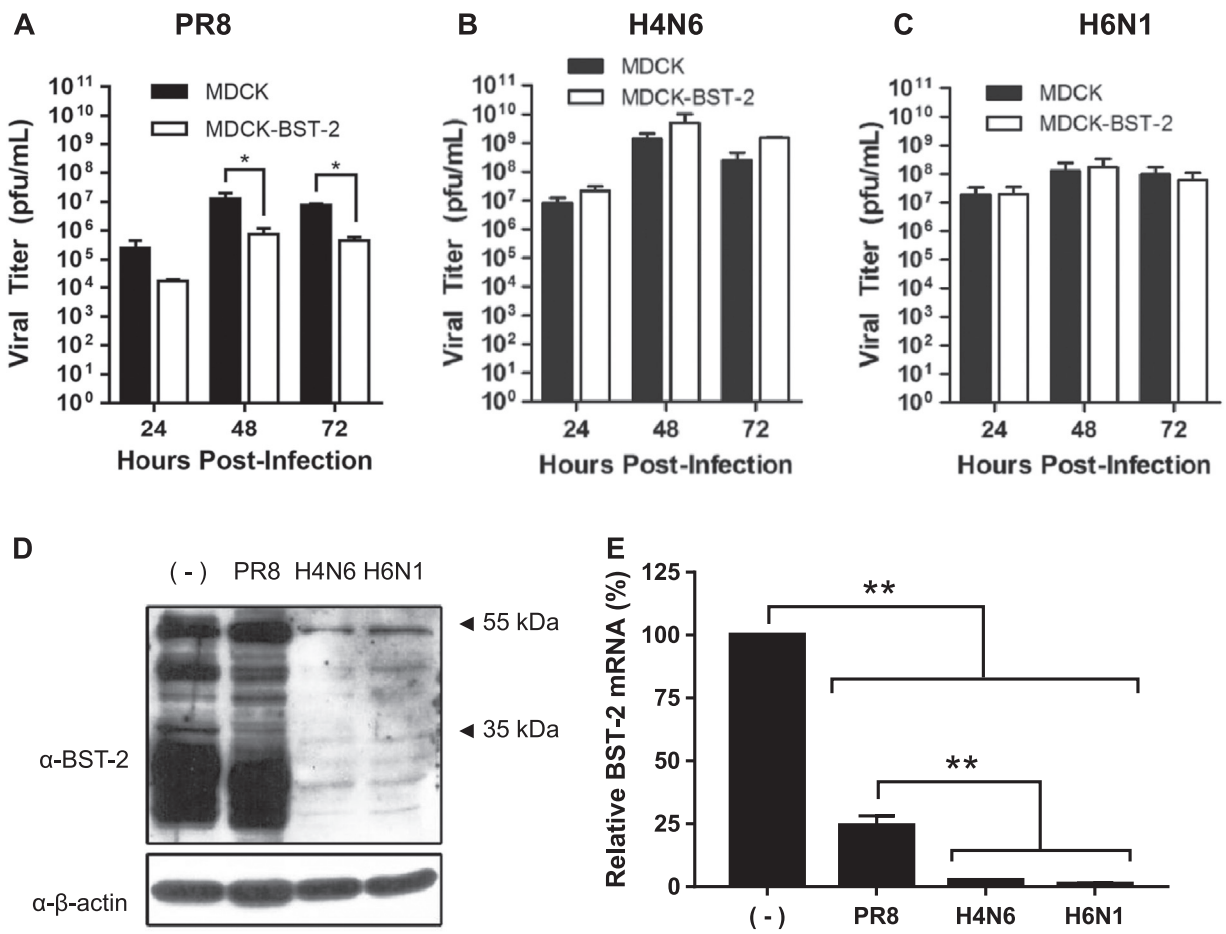

Fig. 2. Viral infection of MDCK and MDCK-BST-2 cell lines. MDCK and MDCK-BST-2 cells were separately seeded in 6-well plates. The cells were infected with PR8, H4N6 or H6N1 virus at an MOI of 0.001 in the presence of 1 μg/mL TPCK-treated trypsin. (A–C) Supernatants were collected at the indicated time points and used to infect MDCK cells for plaque titration. (D) MDCK-BST-2 cell lysates were collected 48 h post-infection and analyzed by western blotting by probing for BST-2 and β-actin. (E) MDCK-BST-2 cells were plated in 6-well plates and either left uninfected or infected with the indicated viruses at an MOI of 1 in the absence of TPCK-treated trypsin. Cells were harvested after 24 h and assessed for relative BST-2 mRNA levels by RT-qPCR. (−), mock infection; *, $p < 0.05$; **, $p < 0.005$.

levels with PA gene segments from other influenza virus strains, namely the pandemic A/Nonthaburi/102/2009 (H1N1), A/Uruguay/716/2007 (H3N2), and A/open-billed stork/Bangkok/LBD0511F/2004 (H5N1). Among all the PA genes tested, the low pathogenic avian influenza viruses H4N6 and H6N1 resulted in the most significant decrease in BST-2 protein levels (Fig. 3D, Supplementary Fig. 2A). The pandemic H1N1 strain (Non), which has an avian-derived PA, along with the highly pathogenic H5N1 PA, had a noticeable, albeit very mild, effect on BST-2 levels. The PR8 and H3N2 viruses had little observable impact on BST-2 levels. PA protein levels roughly corresponded to their effect on BST-2 levels; H4N6 and H6N1 had the greatest amounts of PA protein, followed by the highly pathogenic H5N1 and the pandemic H1N1. PR8 and H3N2 PA levels were notably lower, likely due to the presence of BST-2 itself, which has been previously shown to decrease expression of co-transfected genes (Narkpuk et al., 2014). Indeed, in the absence of BST-2, PA of PR8 and the H3N2 and H5N1 viruses were expressed at higher levels, whereas H4N6 and H6N1 PA were expressed at lower levels (Fig. 3E). These results suggest that the H4N6 and H6N1 PA-mediated down-regulation of BST-2 may pre-empt BST-2 activity, preventing BST-2 from decreasing PA expression.

2.4. PA-X ORF is involved in BST-2 down-regulation

The main product of the PA segment is the PA protein, which functions as an endonuclease (Fodor et al., 2002; Hara et al., 2006). Interestingly, this segment also encodes an alternative product, PA-X, containing the N-terminal endonuclease domain of PA fused to a frameshifted C-terminal tail (Jagger et al., 2012). PA-X has been demonstrated to actively target host RNA polymerase II-derived transcripts for cleavage (Khaperskyy et al., 2016) and is thought to play a role in decreasing host competition for resources as well as down-regulating host responses (Hayashi et al., 2015; Jagger et al., 2012). In addition, it displays host- and strain-specific impact on influenza virus pathogenicity and transmissibility (Hu et al., 2018). To dissect the roles of both PA segment products in mediating BST-2 down-regulation, we mutated the PA segment based on work by Jagger et al., which had identified the frameshift motif (UCC UUU CGU C; Fig. 4A) required for PA-X expression as well as narrowed down the essential residues to 3 positions that resulted in under 0.1% frameshifting efficiency when mutated (UCC UUU CGU C to UCC UUC AGA C) (Jagger et al., 2012). They also generated a single C nucleotide deletion mutant (UCC UUU CGU C to UCC UUU –GU C) which shifted the PA-X ORF (open reading frame) into a position in-frame with the start codon, resulting in expression of PA-X but not PA.

We emulated their mutagenesis approach for PR8 and the H6N1 virus (Fig. 4B), mutating the frameshift motif to either reduce frameshifting into the PA-X ORF (FS) or to force expression solely in the PA-X ORF (ΔC), and assessed which ORF is responsible for the observed decreases in BST-2 levels. Wild-type or mutant PA was co-transfected with a BST-2 expression plasmid into HEK293T cells, and cell lysates were harvested for western blot analysis (Fig. 4C, Supplementary Fig. 2B). As seen previously, the H6N1 wild-type PA decreased BST-2 levels to a

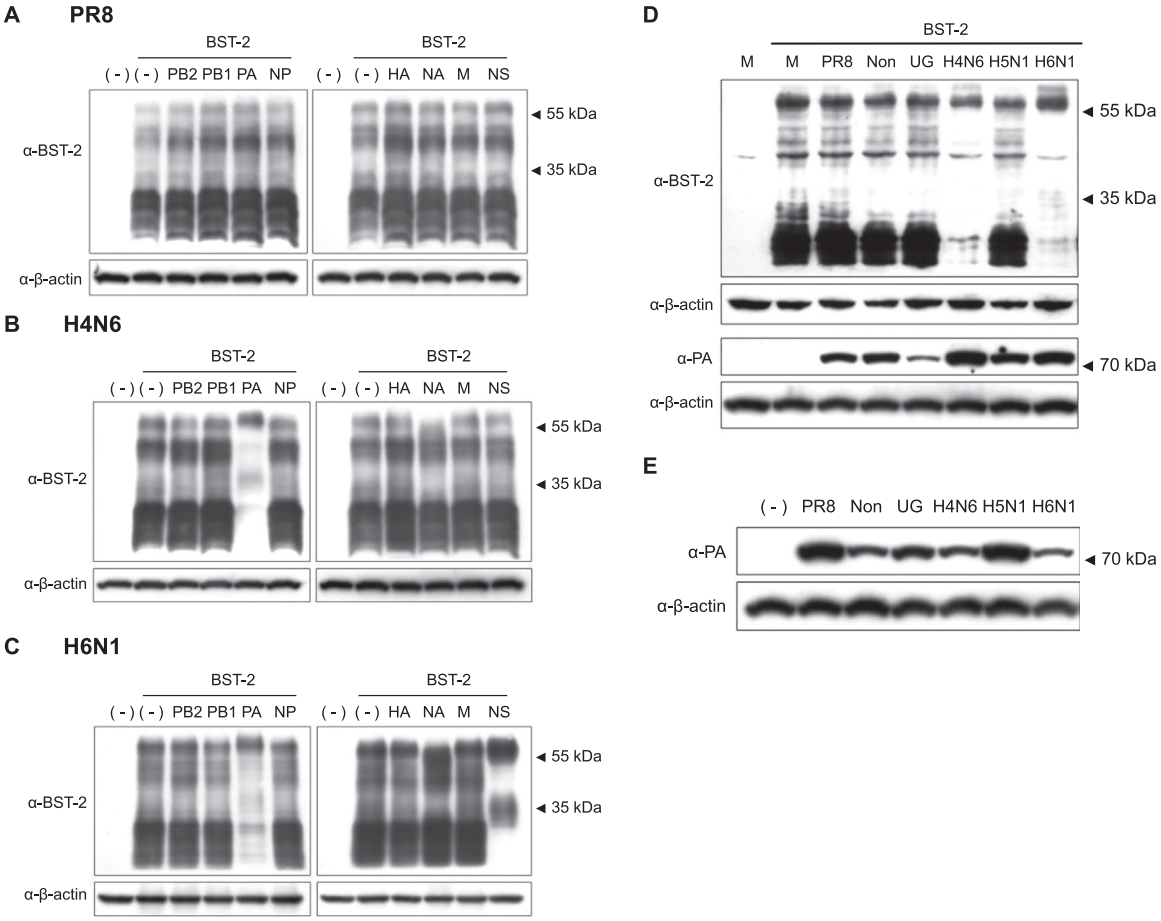

Fig. 3. Impact of individual influenza virus segments on BST-2 expression. (A–C) The eight reverse genetics plasmids of (A) PR8, (B) H4N6, or (C) H6N1 viruses were individually transfected along with the BST-2 expression plasmid into HEK293T cells seeded in 6-well plates. Cells were harvested 72 h post-transfection and cell lysates were analyzed by western blotting by probing for BST-2 and β-actin. (D–E) Plasmids encoding the PA of various influenza virus strains were transfected (D) in the presence or (E) absence of BST-2 into HEK293T cells seeded in 6-well plates. Cells were harvested 72 h post-transfection and cell lysates were analyzed by western blotting by probing for PA, BST-2, and β-actin. (−), mock transfection; Non, A/Nonthaburi/102/2009 (H1N1); UG, A/Uruguay/716/2007 (H3N2); H5N1, A/open-billed stork/Bangkok/LBD0511F/ 2004 (H5N1).

much greater extent than the PR8 wild-type PA. The H6N1 ΔC PA, which is frameshifted to express only the PA-X ORF, resulted in undetectable levels of BST-2 while the FS PA lost its activity. These results indicate that the effect of the H6N1 PA segment on BST-2 levels may be attributed to the PA-X ORF. Similarly, the PR8 ΔC mutant decreased BST-2 levels while the FS mutant had no effect, further demonstrating that the PR8 PA-X ORF also has the ability to decrease BST-2 protein levels in transfected cells. However, because PR8 wild-type and ΔC PA both exhibit less down-regulation of BST-2 protein compared to its H6N1 counterparts, we surmise that PR8 PA-X expression levels or activity may be lower.

2.5. Avian PA relieves BST-2 restriction during infection

Since our observations demonstrated impact of the avian PA segment on BST-2 down-regulation in the context of transfection, we were interested in examining whether or not such impact translated to viral growth in the context of infection. First, we generated chimeric PR8 and H6N1 viruses where the PA, NS or both PA and NS segments were swapped, as well as PR8 and H6N1 viruses carrying the FS mutation in their PA segments. MDCK-BST-2 cells were infected with these viruses at an MOI of 0.001, and cell lysates were assessed for BST-2 and viral NP (nucleoprotein) expression (Fig. 5A, Supplementary Fig. 2C). The PR8-based chimeras carrying H6N1 NS and/or wild-type PA were capable of decreasing BST-2 levels, with the strongest impact being seen with the wild-type PA segment alone. The PR8 viruses with FS PA, either its own or that of H6N1, did not exhibit BST-2 down-regulation. On the other hand, the H6N1 chimeric viruses carrying either the PR8 wild-type PA or both PR8 NS and wild-type PA completely lost their ability to decrease BST-2 levels. The H6N1 FS mutant lost most of their activity, while the virus carrying PR8 NS lost some activity but still yielded noticeably decreased BST-2 levels. These results suggest that H6N1 PA plays the primary role in down-regulating BST-2, with some contribution from its NS segment. Interestingly, the presence of both H6N1 NS and wild-type PA in PR8 did not result in an additive effect on BST-2 levels, but rather resulting in a weaker effect on BST-2 than H6N1 wild-type PA alone. This suggests that viral context also plays a role in how PA and NS manifest their BST-2 antagonism.

To examine the role of the PA segment further, we infected MDCK-BST-2 cells at an MOI of 5 and incubated the cells for 18 h in the absence of TPCK-treated trypsin to limit the viruses to a single round of growth. This would allow us to examine the impact of viral infection on BST-2 levels without being confounded by differences in viral spread due to variable BST-2 sensitivity. Western blotting results reflect our transfection observations, although to a less dramatic extent (Fig. 5B, Supplementary Fig. 2D), likely due to the single-round nature of these infections. The H6N1 virus resulted in the lowest BST-2 levels, followed by PR8 (H6N1 PA), the PR8 virus carrying the H6N1 PA segment. BST-2 mRNA levels were also examined (Fig. 5C). Loss of frameshifting into the PA-X ORF resulted in notable losses in the ability to down-regulate BST-2 mRNA, strongly suggesting a role for PA-X in controlling BST-2 transcription. However, swapping the PA segment as a whole did not

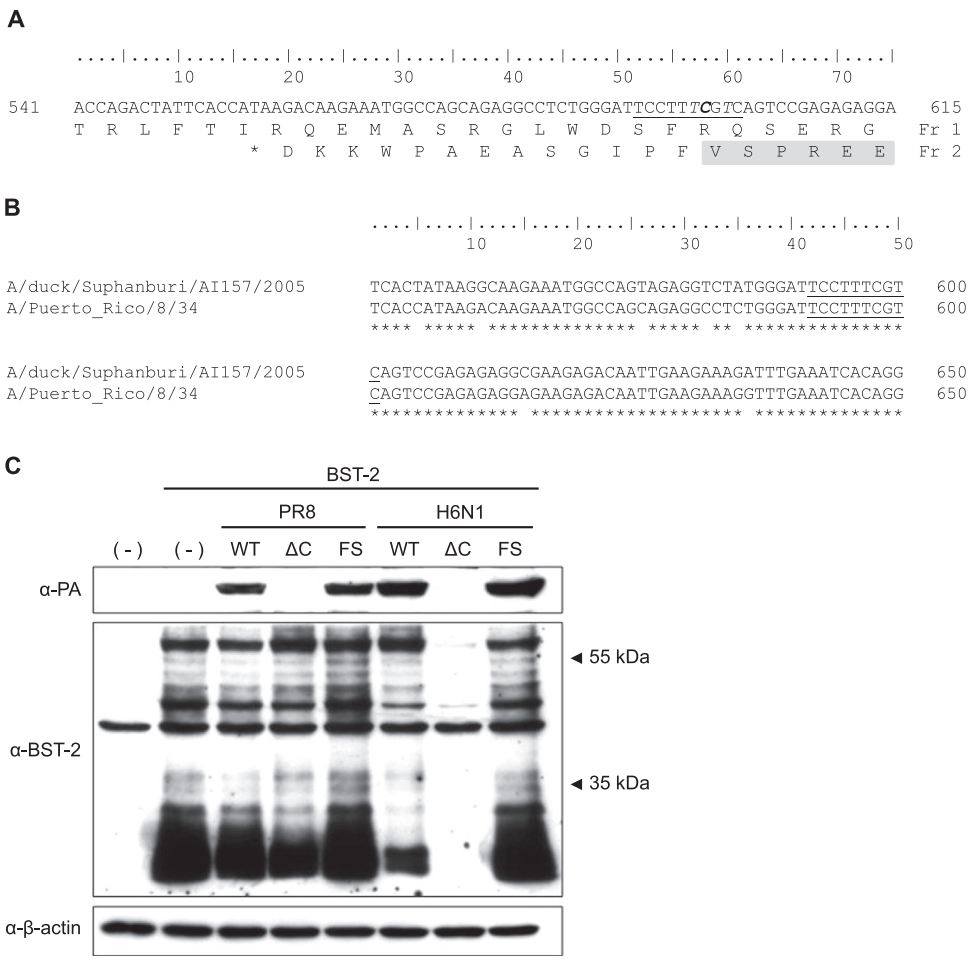

Fig. 4. Impact of PA frameshifting on BST-2 expression. (A) A portion of the N-terminal nucleotide sequence of the PR8 PA segment (541–615) is shown, along with the amino acid translations in frames 1 and 2. The frameshift motif is underlined. Italics indicate the FS mutations in the frameshift motif. Bold indicates the C deletion used to shift the reading frame to the PA-X ORF. The highlighted amino acid residues indicate the beginning of the PA-X tail encoded by the PA-X ORF. (B) Sequence alignment of the N-terminal region of PR8 (A/Puerto Rico/8/34) and H6N1 (A/duck/Suphanburi/AI157/2005). The conserved frameshift motif is underlined. (C) HEK293T cells were plated in 6-well plates and co-transfected with BST-2 along with various PA constructs derived from the PR8 and H6N1 viruses. Cells were harvested 72 h post-transfection and cell lysates were analyzed by western blotting by probing for PA, BST-2, and β-actin. (−), mock transfection; WT, wild-type PA; ΔC, C-deletion mutant; FS, frameshift motif mutant.

affect BST-2 mRNA levels significantly. Considering the impact of the PA segment on BST-2 protein levels (Fig. 5A and B), this appears to indicate a distinct role for the PA segment as a whole in BST-2 protein down-regulation.

To assess the role of the PA segment in rescuing viral replication in the presence of BST-2, we assessed the growth kinetics of PR8 (H6N1 PA) and H6N1 (PR8 PA) alongside the wild-type viruses (Fig. 5 D–G). MDCK or MDCK-BST-2 cells were infected and their supernatants were harvested at various time points for plaque titration on MDCK cells. The growth kinetics data for the wild-type viruses reflect those observed previously, with PR8 exhibiting sensitivity to BST-2 while H6N1 replicated similarly in both MDCK and MDCK-BST-2 cells. With the chimeric viruses, the H6N1 PA was able to confer BST-2 resistance to PR8, while H6N1 (PR8 PA) was rendered sensitive to BST-2. All together, our data suggest that the PA segment carries the determinants for BST-2 resistance in our study system, with the avian H6N1 PA antagonizing BST-2 by down-regulating its expression at both mRNA and protein levels.

3. Discussion

Several studies have examined the impact of BST-2 on influenza virus replication, and a handful of viral proteins have been proposed as possible antagonists of human BST-2. Given the zoonotic nature of influenza viruses, we were interested in exploring this question from the perspective of human BST-2 acting as a cross-species transmission barrier for avian influenza viruses. We report here that, contrary to our initial hypothesis that low pathogenic avian influenza viruses incapable of transmission to human hosts would be strongly restricted by human BST-2, H4N6 and H6N1 viruses grew to robust titers in MDCK cells constitutively expressing BST-2 and appeared completely resistant to its antiviral activity. Mechanistically, our data suggest that this resistance is likely conferred by the drastic down-regulation of BST-2 levels by the avian PA segment through the reported ability of PA-X to mediate general host shut-off (Jagger et al., 2012).

Before discussing the implications of our PA-associated findings, it is important to note that the H6N1 NS segment also exhibited the ability to decrease BST-2 protein levels. Unlike PR8, this H6N1 virus contains the F103 and M106 residues in its NS1 protein that are associated with host CPSF30 (30-kDa subunit of the cleavage and polyadenylation specificity factor) interaction and NS1-mediated host-shut-off (Das et al., 2008). CPSF30 interaction may not be directly related to BST-2 down-regulation or the sole contributor to this effect, however, as the H4N6 virus also carries this motif despite having an NS segment that did not decrease BST-2 protein levels. The H4N6 NS1 protein is divergent from H6N1 NS1 at five positions, carrying K20, I129, I137, A155, and S165 instead of R20, T129, N137, V155, and F165. Interestingly, three of these distinct H4N6 NS1 residues are shared with PR8, namely those at positions 129, 155, and 165. Residue 165, in particular, is located in the SH3 binding motif 1 that is involved in interaction with the PI3K (phosphatidylinositol 3-kinase) p85β subunit (Shin et al., 2007). While we did not extensively examine the role of NS1 nor these residues in the down-regulation of BST-2, NS1 of A/WSN/33 (H1N1) and A/Texas/36/91 were previously reported to prevent the induction of BST-2 upon IFN-α treatment (Mangeat et al., 2012). This effect is not evident in most influenza virus–BST-2 studies which have focused on engineered cell lines constitutively expressing BST-2 (Bruce et al., 2012; Winkler et al., 2012). Even so, our data revealed a strain-specific ability of NS1 to decrease BST-2 levels during infection in such a cell line, supporting the diversity of NS1 functionality in modulating the host

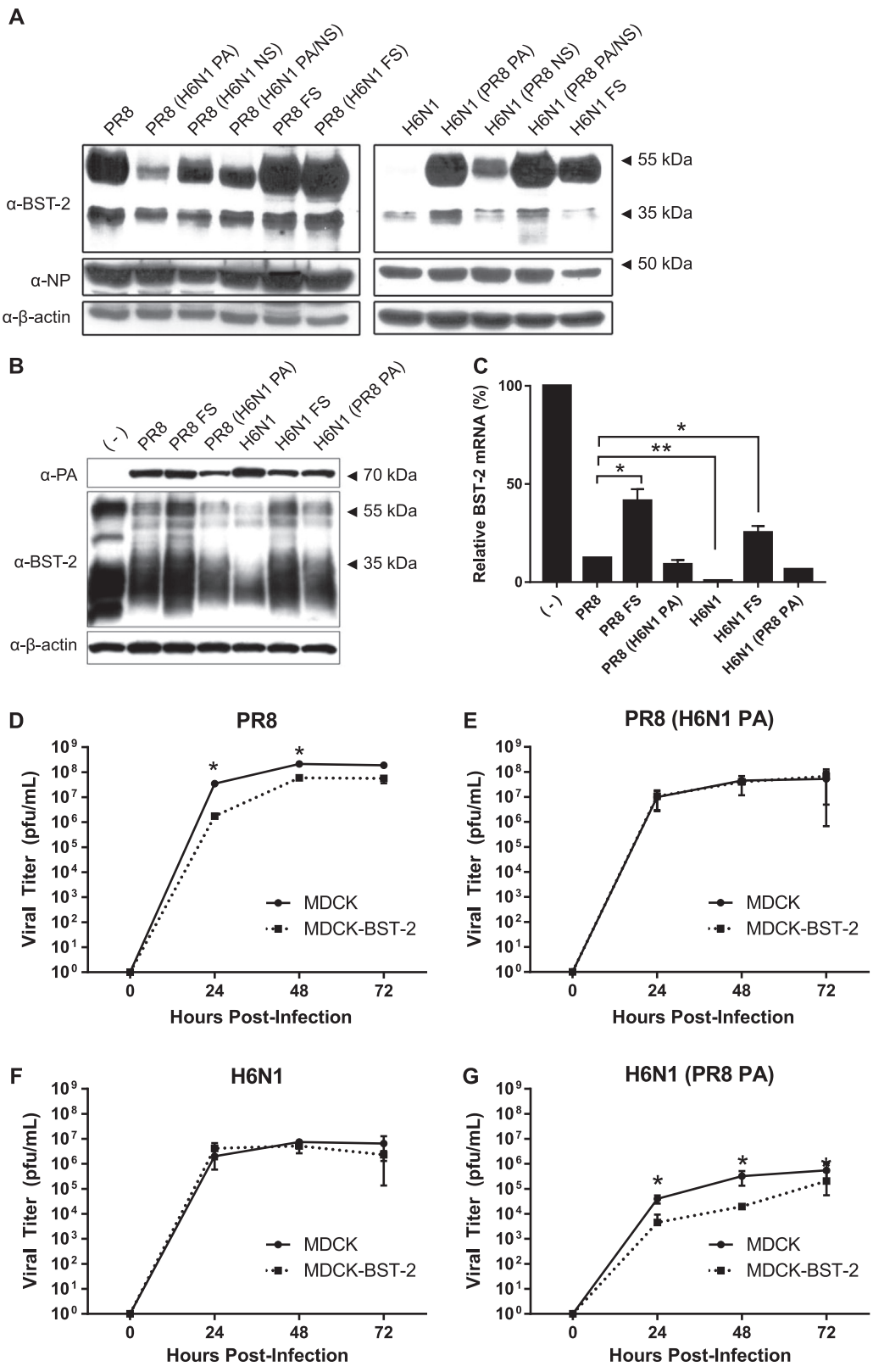

Fig. 5. Chimeric virus infection of MDCK-BST-2. (A) MDCK-BST-2 cells were seeded in 6-well plates and infected with the indicated reverse genetics-derived viruses at an MOI of 0.001. Cells were harvested 72 h post-infection and analyzed by western blotting by probing for NP, BST-2, and β-actin. (B–C) MDCK-BST-2 cells were infected with viruses at an MOI of 5. Cells were harvested 18 h after infection in the absence of TPCK-trypsin and analyzed by (B) western blotting by probing for PA, BST-2, and β-actin, or (C) by RT-qPCR for BST-2 mRNA levels. Mock-infected MDCK-BST-2 mRNA level was set as 100%. (D–G) MDCK and MDCK-BST-2 cells were infected with the indicated viruses at an MOI of 0.001 and supernatants were collected at various time points post-infection. Viral growth was quantified by plaque titration on MDCK cells. (−), mock infection; *, $p < 0.05$; **, $p < 0.005$.

innate immune response beyond its role in IFN suppression. The other products of the NS segment, NEP (nuclear export protein) and NS3 are unlikely to be associated with the observed impact of H6N1 NS on BST-2, however. The NS3 splicing motif, an A to G mutation at nucleotide position 374 (Selman et al., 2012), is not present in any of the three viruses, while the NEP protein sequence is perfectly conserved between the H4N6 and H6N1 viruses.

Additionally, while we focused primarily on the PA segment, our results do not rule out the possibility that other viral proteins encoded on two or more segments may work in concert in order to effect BST-2 decrease, as previously seen with NA and HA (Gnirss et al., 2015; Hu et al., 2015). Neither do these results discount the presence of other

anti-BST-2 mechanisms involved in sequestering or altering BST-2 localization, which would thereby decrease the impact of BST-2 on influenza virus replication through means other than direct down-regulation of BST-2 expression as assessed by mRNA and protein levels.

Early on during this work, we hypothesized that PA-X, first described in 2012 by Jagger et al. (2012) as a frameshift product of the PA gene with endonuclease and host shut-off activity, might be responsible for BST-2 down-regulation as both protein and mRNA levels were affected. Indeed, in the transfection studies, the PA-X ORF appears to be strongly involved in mediating the decrease in BST-2 expression levels. This effect was likely due to endonuclease-mediated cleavage of RNA, preventing protein translation. Likewise, decreases in both BST-2 mRNA and protein were observed in infected cells. Suppression of BST-2 mRNA during infection that has previously been reported (Mangeat et al., 2012) could likely also be explained by the effect of the PA segment as well. However, the interpretation of PA and PA-X ORF involvement in BST-2 down-regulation changes slightly in the context of infection, as BST-2 is pre-expressed in the MDCK-BST-2 cell line. The ability of H4N6 and H6N1 infection to reduce both BST-2 mRNA and protein levels suggest that there is either post-translational down-regulation or extremely rapid turnover of BST-2, or both. If the former effect is indeed the case, it would be interesting to map out the mechanism by which PA-X may have exerted such a dramatic effect on protein stability. Nevertheless, our infection studies (Figs. 2 and 5) show a distinct difference between BST-2 mRNA and protein levels in PR8-infected cells, where mRNA levels are decreased but protein levels are not. This suggests that the endonuclease and protein down-regulation activities may be distinct. Alternatively, the impact of mRNA degradation may be amplified at a certain threshold due to high BST-2 turnover.

In our transfection experiments with mutant PA, we found that the H6N1 wild-type PA exhibited a BST-2 restriction phenotype similar to the ΔC PA mutant which expresses only the PA-X ORF, whereas the PR8 wild-type PA phenotype was reflected in the FS PA mutant. These observations suggest that the PA-X ORF may be fundamentally different between the two viruses. It is possible that the H6N1 PA-X protein is expressed at very high levels from the wild-type PA gene, similar to that of the ΔC mutant. This in turn implies that expression of the full-length PA protein itself may suffer as a result, due to higher rates of ribosomal frameshifting during translation. In other words, H6N1 and PR8 PA may differ in frameshifting rates as determined by factors outside the identified, highly-conserved frameshift motif. Alternatively, activity of their PA-X may be different despite neither having a truncated PA-X associated with changes in protein activity (Bavagnoli et al., 2015; Gao et al., 2015).

The significance of the PA-X ORF was further highlighted in our attempts to rescue the H4N6 virus. This virus was not used in the later viral mutagenesis studies because we could not rescue it through reverse genetics in MDCK cells. Intriguingly, we were able to successfully rescue one virus: the H4N6 FS mutant carrying the frameshift motif mutation in the PA gene, shown previously to decrease PA-X expression (Jagger et al., 2012). That this mutation was able to render the recombinant H4N6 virus rescuable in cell culture suggests a role for the PA-X ORF in modulating viral growth. Indeed, PA-X has been described to suppress viral polymerase activity in certain contexts (Gong et al., 2017; Hu et al., 2015), and its loss was accordingly associated with increased viral replication in both tissue culture and infected animals. It is tempting to speculate that this shifting of balance between polymerase activity and host shut-off may play some role in host tropism and cross-species transmission.

A recent publication by Hu et al. describes a very similar study to the work we have reported here (Hu et al., 2017). From the observation that infection by A/WSN/33 (H1N1) reduced BST-2 levels, they assessed the major viral proteins individually for their effect on BST-2 expression and identified M2 as responsible for BST-2 down-regulation. While we did not specifically separate M1 and M2 expression in our study, the M segments of PR8, H4N6, and H6N1 as a whole did not confer BST-2 down-regulation. Similarly, Bruce et al. tested M2-deficient PR8 and found that loss of M2 did not notably affect alter its sensitivity to BST-2 (Bruce et al., 2012). On the other hand, Hu et al. did not observe any impact of PA on BST-2 levels; this indicates that A/WSN/33 PA may be similar to that of PR8, whose PA also lacks the activity seen with H4N6 and H6N1 viruses. These disparate, seemingly contradictory results actually point towards a single conclusion—that influenza A resistance to and antagonism of BST-2 is strain-specific, and that the role of the PA segment may possibly be associated with low pathogenic avian strains.

4. Conclusion

Overall, our data further elaborate upon the interaction between the antiviral protein BST-2 and influenza viruses. We identified the PA segment as a species-specific determinant of sensitivity to BST-2, with those of low pathogenic avian influenza viruses exhibiting the ability to down-regulate human BST-2 in both transfection and infection contexts. That such drastic impact was seen even with high levels of pre-expressed protein that cannot be controlled pre-translationally by NS1 suggests that BST-2 does not necessarily act as a cross-species barrier for transmission of low pathogenic avian influenza viruses to humans. Furthermore, as these effects were surprisingly not observed to the same extent with tested human and human-derived viruses, we hypothesize that the avian PA segment may exhibit a different PA–PA-X balance that would translate into a disproportionately large impact on balancing host-shut off with viral replication compared to human viruses.

5. Materials and methods

5.1. Cells and viruses

Human embryonic kidney (HEK) 293T and Madin-Darby canine kidney (MDCK) cells were maintained in Opti-MEM (Life Technologies) supplemented with 10% fetal bovine serum (FBS). Cells were passaged twice weekly by detaching with 0.25% trypsin, and kept in a 37 °C incubator at 5% CO_2.

Influenza viruses, and their proteins, studied in this work comprise A/Puerto Rico/8/34 (H1N1) (PR8) and A/duck/Hong Kong/365/78 (H4N6), gifts from Dr. Robert G. Webster, St. Jude Children's Research Hospital, Tennessee, USA (Hoffmann et al., 2000); A/Nonthaburi/102/2009 (H1N1) from the Department of Medical Sciences, Ministry of Public Health, Bangkok, Thailand; A/Uruguay/716/2007 (H3N2) from Dr. Sathit Pichyangkul, Armed Forces Research Institute of Medical Sciences, Bangkok, Thailand; and A/open-billed stork/Bangkok/LBD0511F/2004 (H5N1) viral RNA and A/duck/Suphanburi/AI157/2007 (H6N1) from Dr. Arunee Thitithanyanont, Mahidol University, Bangkok, Thailand.

5.2. Generation of cell lines stably expressing BST-2

The human BST-2 coding sequence was amplified from pHW-BST-2 (Narkpuk et al., 2014) with primers carrying the *Bam*HI and *Not*I restriction sites for cloning into the lentiviral vector pSIN-CSGW-UbEm (a gift from Dr. Yasuhiro Ikeda, Mayo Clinic, Minnesota, USA). HEK293T cells were transfected with the lentiviral vector along with VSV-G-expressing pMD-G (Naldini et al., 1996) and the packaging plasmid pCMV-ΔR8.91 (Zufferey et al., 1997), and supernatants containing lentiviral particles were harvested 48 h post-transfection. The supernatants were clarified by centrifugation and used to infect MDCK cells seeded in a 60-mm dish. Polybrene (Sigma-Aldrich) was added to the infectious supernatant at a concentration of 8 μg/mL. Single clones of transduced MDCK cells were prepared and expression of BST-2 by these clones (MDCK-BST-2) was verified by western blotting.

5.3. Immunofluorescence staining

MDCK-BST-2 cells were plated at a density of 5×10^4 cells in a Lab-Tek II chamber slide (Thermo Scientific) and incubated overnight. Cells were washed with phosphate-buffered saline (PBS) and fixed with 4% formaldehyde for 5 min. After washing with PBS, cells were blocked with blocking buffer (PBS supplemented with 10% FBS and 1% BSA) for one hour at room temperature, probed with a 1:1000 dilution of a rabbit anti-BST-2 antibody (Santa Cruz Biotechnology) in blocking buffer for one hour, washed in PBS, and incubated with a 1:1000 dilution of Alexa-488-conjugated goat anti-rabbit IgG (Abcam) for another hour. After a final washing step with PBS, cells were stained with DAPI and imaged by fluorescence microscopy.

5.4. Generation of H4N6 and H6N1 reverse genetics plasmids

Viral RNA from the A/duck/Hong Kong/365/78 (H4N6) and A/duck/Suphanburi/AI157/2007 (H6N1) viruses were extracted using the Viral Nucleic Acid Extraction II Kit (Geneaid). The RNA was used as a template for RT-PCR using Takara's One Step RT-PCR kit (Clontech) along with primers containing the *Bsm*BI restriction sites and specific for the 5′ and 3′ untranslated regions of each genomic RNA segment (Hoffmann et al., 2001). Amplified cDNA products were digested with *Bsm*BI and inserted into the pHW2000 vector (Hoffmann et al., 2000). Selected clones were sequenced and compared to the official sequence reports on Genbank. Any nucleotide position that did not match sequence data on Genbank was corrected by site-directed mutagenesis.

PA mutants were generated following the mutagenesis approach reported by Jagger et al. (2012). The ΔC mutants were generated with primers covering the frameshift motif with a single C598 nucleotide deletion. The FS (frameshift) mutants were generated with primers covering the frameshift motif with mutations of residues 597–600 from UCGU to CAGA.

5.5. Virus reverse genetics and propagation

Six-well plates were seeded with co-cultures of 7.5×10^5 HEK293T cells and 2.5×10^5 MDCK cells overnight prior to transfection with eight pHW2000-based plasmids encoding the eight influenza virus genomic segments (500 ng each). Twenty-four hours after transfection, the cells were washed and replenished with serum-free Opti-MEM supplemented with 1 μg/mL TPCK-treated trypsin. Reverse genetics supernatants were harvested once extensive cell death was observed (typically 48 h post-transfection) and clarified by centrifugation at $230 \times g$ prior to injection into 10-day old embryonated chicken eggs. The eggs were incubated at 37 °C for 48 h before the allantoic fluid was collected for virus. Allantoic fluid was clarified by centrifugation at $230 \times g$ and sterilized by passage through a 0.20 μm syringe filter before storage at −80 °C.

To verify the sequence of these reverse genetics-derived viruses, RNA from the viruses were extracted using the Viral Nucleic Acid Extraction II Kit. RT-PCR was performed using the Superscript III One-Step RT-PCR System (Invitrogen) and the products were then submitted for sequencing (1st Base, Malaysia).

5.6. Viral infection

To study growth kinetics, MDCK or MDCK-BST-2 cells were plated at a density of 5×10^5 cells per well in 6-well plates overnight and infected with virus at an MOI of 0.001. After an hour of virus adsorption at 37 °C, the cells were washed with PBS and replenished with serum-free Opti-MEM supplemented with 1 μg/mL TPCK-treated trypsin. Supernatant samples were collected at various times points for plaque titration. To assess the impact of chimeric and mutant viruses on BST-2 expression, an MOI of 5 was used for infection and cells were incubated in the absence of TCPK-treated trypsin for 18 h prior to harvest.

5.7. Plaque titration

MDCK cells were plated at a density of 8×10^5 cells per well in 6-well plates and incubated overnight. Influenza viruses from cell culture supernatants were prepared as serial 10-fold dilutions and appropriate dilutions added to seeded cells. Cells were incubated at 37 °C for 1 h and then washed with PBS before being overlaid with agar in minimum essential medium (MEM) supplemented with 1 μg/mL TPCK-treated trypsin. After another 48–72 h at 37 °C, the agar was removed and the cells fixed with 0.1% crystal violet in formaldehyde. Viral titers were calculated by counting the number of plaques in the well containing 10–100 plaques and then multiplying that number by the dilution factor. Log transformation was applied to viral titer readouts prior to assessment of statistical significance with Student's two-tailed *t*-test.

5.8. Western blotting

Infected or transfected cells were lysed in radioimmunoprecipitation (RIPA) buffer (50 mM Tris-Cl pH 7.4, 120 mM NaCl, 1% Triton X-100, 0.5% sodium deoxycholate, 1% sodium dodecyl sulfate) supplemented with 1% ProteoBlock Protease Inhibitor Cocktail (Thermo Scientific)). Lysates were loaded into 10 or 12% polyacrylamide gels for SDS-PAGE, and subsequently transferred onto nitrocellulose membranes. Membranes were blocked with 5% skim milk in 0.1% Tween 20–Tris-buffered saline (TBS) for at least one hour before probing with antibody. Human BST-2 was detected with a rabbit anti-human BST-2 antibody (Santa Cruz Biotechnology), influenza virus PA with a rabbit anti-PA antibody (Thermo Scientific), and β-actin with a mouse anti-β-actin antibody (Santa Cruz Biotechnology). Secondary antibodies (horseradish peroxidase-conjugated goat anti-rabbit IgG and goat anti-mouse IgG antibodies) were purchased from Santa Cruz Biotechnology. Bands were visualized using the Clarity Western ECL Substrate chemiluminescence kit (Bio-Rad) by film exposure. Films were scanned using the Molecular Imager ChemiDoc XRS + Imaging System (Bio-Rad) and analyzed by densitometry using ImageJ.

5.9. Quantitative PCR

Infected MDCK and MDCK-BST-2 cells were harvested in PBS at various time points. Half the harvested cells were used for genomic DNA extraction using the GeneJet Genomic DNA Purification Kit (Thermo Scientific), and the remaining half used for RNA extraction using the GeneJet RNA Purification Kit (Thermo Scientific). Extractions were carried out according to manufacturer instructions. Quantitative PCR (qPCR) was performed on the genomic DNA to assess relative fibronectin copy number using the SSOAdvanced Universal SYBR Green Supermix (Bio-Rad) and the two-step qPCR protocol according to manufacturer instructions. RT-qPCR was used to assess mRNA levels of the human BST-2 transgene using the iTaq Universal SYBR Green One-Step Kit (Bio-Rad) and the associated two-step protocol according to manufacturer instructions. The Bio-Rad C1000 Touch Thermal Cycler was used to run these qPCR experiments. Statistical significance was assessed with Student's two-tailed *t*-test.

Acknowledgements

We thank the members of the Virology and Cell Technology Laboratory for their insightful comments and critique. This work was funded by the Young Fellow Grant from the National Center for Genetic Engineering and Biotechnology (BIOTEC), Thailand. The authors declare no conflict of interest.

Appendix A. Supplementary material

Supplementary data associated with this article can be found in the online version at doi:10.1016/j.virol.2018.09.016.

References

Bavagnoli, L., Cucuzza, S., Campanini, G., Rovida, F., Paolucci, S., Baldanti, F., Maga, G., 2015. The novel influenza A virus protein PA-X and its naturally deleted variant show different enzymatic properties in comparison to the viral endonuclease PA. Nucleic Acids Res. 43, 9405–9417.

Bruce, E.A., Abbink, T.E., Wise, H.M., Rollason, R., Galao, R.P., Banting, G., Neil, S.J., Digard, P., 2012. Release of filamentous and spherical influenza A virus is not restricted by tetherin. J. Gen. Virol. 93, 963–969.

Das, K., Ma, L.C., Xiao, R., Radvansky, B., Aramini, J., Zhao, L., Marklund, J., Kuo, R.L., Twu, K.Y., Arnold, E., Krug, R.M., Montelione, G.T., 2008. Structural basis for suppression of a host antiviral response by influenza A virus. Proc. Natl. Acad. Sci. USA 105, 13093–13098.

Evans, D.T., Serra-Moreno, R., Singh, R.K., Guatelli, J.C., 2010. BST-2/tetherin: a new component of the innate immune response to enveloped viruses. Trends Microbiol. 18, 388–396.

Fodor, E., Crow, M., Mingay, L.J., Deng, T., Sharps, J., Fechter, P., Brownlee, G.G., 2002. A single amino acid mutation in the PA subunit of the influenza virus RNA polymerase inhibits endonucleolytic cleavage of capped RNAs. J. Virol. 76, 8989–9001.

Gao, H., Sun, H., Hu, J., Qi, L., Wang, J., Xiong, X., Wang, Y., He, Q., Lin, Y., Kong, W., Seng, L.G., Pu, J., Chang, K.C., Liu, X., Liu, J., Sun, Y., 2015. Twenty amino acids at the C-terminus of PA-X are associated with increased influenza A virus replication and pathogenicity. J. Gen. Virol. 96, 2036–2049.

Gnirss, K., Zmora, P., Blazejewska, P., Winkler, M., Lins, A., Nehlmeier, I., Gartner, S., Moldenhauer, A.S., Hofmann-Winkler, H., Wolff, T., Schindler, M., Pohlmann, S., 2015. Tetherin sensitivity of influenza A viruses is strain specific: role of hemagglutinin and neuraminidase. J. Virol. 89, 9178–9188.

Gong, X.Q., Sun, Y.F., Ruan, B.Y., Liu, X.M., Wang, Q., Yang, H.M., Wang, S.Y., Zhang, P., Wang, X.H., Shan, T.L., Tong, W., Zhou, Y.J., Li, G.X., Zheng, H., Tong, G.Z., Yu, H., 2017. PA-X protein decreases replication and pathogenicity of swine influenza virus in cultured cells and mouse models. Vet. Microbiol. 205, 66–70.

Hara, K., Schmidt, F.I., Crow, M., Brownlee, G.G., 2006. Amino acid residues in the N-terminal region of the PA subunit of influenza A virus RNA polymerase play a critical role in protein stability, endonuclease activity, cap binding, and virion RNA promoter binding. J. Virol. 80, 7789–7798.

Hayashi, T., MacDonald, L.A., Takimoto, T., 2015. Influenza A virus protein PA-X contributes to viral growth and suppression of the host antiviral and immune responses. J. Virol. 89, 6442–6452.

Heusinger, E., Kluge, S.F., Kirchhoff, F., Sauter, D., 2015. Early vertebrate evolution of the host restriction factor tetherin. J. Virol. 89, 12154–12165.

Hoffmann, E., Neumann, G., Kawaoka, Y., Hobom, G., Webster, R.G., 2000. A DNA transfection system for generation of influenza A virus from eight plasmids. Proc. Natl. Acad. Sci. USA 97, 6108–6113.

Hoffmann, E., Stech, J., Guan, Y., Webster, R.G., Perez, D.R., 2001. Universal primer set for the full-length amplification of all influenza A viruses. Arch. Virol. 146, 2275–2289.

Hu, J., Ma, C., Liu, X., 2018. PA-X: a key regulator of influenza A virus pathogenicity and host immune responses. Med. Microbiol. Immunol.

Hu, J., Mo, Y., Wang, X., Gu, M., Hu, Z., Zhong, L., Wu, Q., Hao, X., Hu, S., Liu, W., Liu, H., Liu, X., 2015. PA-X decreases the pathogenicity of highly pathogenic H5N1 influenza A virus in avian species by inhibiting virus replication and host response. J. Virol. 89, 4126–4142.

Hu, S., Yin, L., Mei, S., Li, J., Xu, F., Sun, H., Liu, X., Cen, S., Liang, C., Li, A., Guo, F., 2017. BST-2 restricts IAV release and is countered by the viral M2 protein. Biochem. J. 474, 715–730.

Jagger, B.W., Wise, H.M., Kash, J.C., Walters, K.A., Wills, N.M., Xiao, Y.L., Dunfee, R.L., Schwartzman, L.M., Ozinsky, A., Bell, G.L., Dalton, R.M., Lo, A., Efstathiou, S., Atkins, J.F., Firth, A.E., Taubenberger, J.K., Digard, P., 2012. An overlapping protein-coding region in influenza A virus segment 3 modulates the host response. Science 337, 199–204.

Jouvenet, N., Neil, S.J., Zhadina, M., Zang, T., Kratovac, Z., Lee, Y., McNatt, M., Hatziioannou, T., Bieniasz, P.D., 2009. Broad-spectrum inhibition of retroviral and filoviral particle release by tetherin. J. Virol. 83, 1837–1844.

Kaletsky, R.L., Francica, J.R., Agrawal-Gamse, C., Bates, P., 2009. Tetherin-mediated restriction of filovirus budding is antagonized by the Ebola glycoprotein. Proc. Natl. Acad. Sci. USA 106, 2886–2891.

Khaperskyy, D.A., Schmaling, S., Larkins-Ford, J., McCormick, C., Gaglia, M.M., 2016. Selective degradation of host RNA polymerase II transcripts by influenza A virus PA-X host shutoff protein. PLoS Pathog. 12, e1005427.

Kupzig, S., Korolchuk, V., Rollason, R., Sugden, A., Wilde, A., Banting, G., 2003. Bst-2/HM1.24 is a raft-associated apical membrane protein with an unusual topology. Traffic 4, 694–709.

Leyva-Grado, V.H., Hai, R., Fernandes, F., Belicha-Villanueva, A., Carter, C., Yondola, M.A., 2014. Modulation of an ectodomain motif in the influenza A virus neuraminidase alters tetherin sensitivity and results in virus attenuation in vivo. J. Mol. Biol. 426, 1308–1321.

Mangeat, B., Cavagliotti, L., Lehmann, M., Gers-Huber, G., Kaur, I., Thomas, Y., Kaiser, L., Piguet, V., 2012. Influenza virus partially counteracts restriction imposed by tetherin/BST-2. J. Biol. Chem. 287, 22015–22029.

Marc, D., 2014. Influenza virus non-structural protein NS1: interferon antagonism and beyond. J. Gen. Virol. 95, 2594–2611.

Naldini, L., Blomer, U., Gallay, P., Ory, D., Mulligan, R., Gage, F.H., Verma, I.M., Trono, D., 1996. In vivo gene delivery and stable transduction of nondividing cells by a lentiviral vector. Science 272, 263–267.

Narkpuk, J., Wanitchang, A., Kramyu, J., Frantz, P.N., Jongkaewwattana, A., Teeravechyan, S., 2014. An unconventional BST-2 function: down-regulation of transient protein expression. Biochem. Biophys. Res. Commun. 450, 1469–1474.

Neil, S.J., Zang, T., Bieniasz, P.D., 2008. Tetherin inhibits retrovirus release and is antagonized by HIV-1 Vpu. Nature 451, 425–430.

Perez-Caballero, D., Zang, T., Ebrahimi, A., McNatt, M.W., Gregory, D.A., Johnson, M.C., Bieniasz, P.D., 2009. Tetherin inhibits HIV-1 release by directly tethering virions to cells. Cell 139, 499–511.

Radoshitzky, S.R., Dong, L., Chi, X., Clester, J.C., Retterer, C., Spurgers, K., Kuhn, J.H., Sandwick, S., Ruthel, G., Kota, K., Boltz, D., Warren, T., Kranzusch, P.J., Whelan, S.P., Bavari, S., 2010. Infectious Lassa virus, but not filoviruses, is restricted by BST-2/tetherin. J. Virol. 84, 10569–10580.

Rivas, H.G., Schmaling, S.K., Gaglia, M.M., 2016. Shutoff of host gene expression in influenza A virus and herpesviruses: similar mechanisms and common themes. Viruses 8, 102.

Sakuma, T., Noda, T., Urata, S., Kawaoka, Y., Yasuda, J., 2009. Inhibition of Lassa and Marburg virus production by tetherin. J. Virol. 83, 2382–2385.

Selman, M., Dankar, S.K., Forbes, N.E., Jia, J.J., Brown, E.G., 2012. Adaptive mutation in influenza A virus non-structural gene is linked to host switching and induces a novel protein by alternative splicing. Emerg. Microbes Infect. 1, e42.

Shin, Y.K., Li, Y., Liu, Q., Anderson, D.H., Babiuk, L.A., Zhou, Y., 2007. SH3 binding motif 1 in influenza A virus NS1 protein is essential for PI3K/Akt signaling pathway activation. J. Virol. 81, 12730–12739.

Taylor, J.K., Coleman, C.M., Postel, S., Sisk, J.M., Bernbaum, J.G., Venkataraman, T., Sundberg, E.J., Frieman, M.B., 2015. Severe acute respiratory syndrome coronavirus ORF7a inhibits bone marrow stromal antigen 2 virion tethering through a novel mechanism of glycosylation interference. J. Virol. 89, 11820–11833.

Van Damme, N., Goff, D., Katsura, C., Jorgenson, R.L., Mitchell, R., Johnson, M.C., Stephens, E.B., Guatelli, J., 2008. The interferon-induced protein BST-2 restricts HIV-1 release and is downregulated from the cell surface by the viral Vpu protein. Cell Host Microbe 3, 245–252.

Wang, M., Zhang, Z., Wang, X., 2018. Strain-specific antagonism of the human H1N1 influenza A virus against equine tetherin. Viruses 10.

Wang, S.M., Huang, K.J., Wang, C.T., 2014. BST2/CD317 counteracts human coronavirus 229E productive infection by tethering virions at the cell surface. Virology 449, 287–296.

Winkler, M., Bertram, S., Gnirss, K., Nehlmeier, I., Gawanbacht, A., Kirchhoff, F., Ehrhardt, C., Ludwig, S., Kiene, M., Moldenhauer, A.S., Goedecke, U., Karsten, C.B., Kuhl, A., Pohlmann, S., 2012. Influenza A virus does not encode a tetherin antagonist with Vpu-like activity and induces IFN-dependent tetherin expression in infected cells. PLoS One 7, e43337.

Yondola, M.A., Fernandes, F., Belicha-Villanueva, A., Uccelini, M., Gao, Q., Carter, C., Palese, P., 2011. Budding capability of the influenza virus neuraminidase can be modulated by tetherin. J. Virol. 85, 2480–2491.

Zufferey, R., Nagy, D., Mandel, R.J., Naldini, L., Trono, D., 1997. Multiply attenuated lentiviral vector achieves efficient gene delivery in vivo. Nat. Biotechnol. 15, 871–875.